

Quantum criticality in Kondo quantum dot coupled to 2D topological insulator

Chung-Hou Chung and Salman Silotri

Electrophysics Department, National Chiao-Tung University, HsinChu, Taiwan, 300, R.O.C.

(Dated: May 16, 2019)

We investigate theoretically the quantum phase transition between the one-channel Kondo (1CK) and two-channel Kondo (2CK) fixed points in a quantum dot coupled to edge states of interacting 2D topological insulators (2DTI) with Luttinger parameter $0 < K < 1$. The model has been studied in Ref.¹⁶, and was mapped onto an anisotropic two-channel Kondo model via bosonization. For $K < 1$, the strong coupling 2CK fixed point was argued to be stable for infinitesimally weak tunnelings between dot and the 2DTI based on the simple scaling dimensional analysis¹⁶. We re-examine the model beyond the scaling dimension analysis via a 1-loop renormalization group (RG) approach on the effective Kondo model via re-fermionization near the 2CK fixed point. We find for $K < 1$ the 2CK fixed point can be unstable towards the 1CK fixed point and the system may undergo a quantum phase transition (QPT) between 1CK and 2CK fixed points. The QPT in our model comes as a result of the combined Kondo and the helical Luttinger physics in 2DTI, and it serves as the first example of the 1CK-2CK QPT that is accessible by the perturbative RG approach. We extract quantum critical and crossover behaviors from various thermodynamical quantities near the quantum critical point.

PACS numbers: 72.15.Qm, 7.23.-b, 03.65.Yz

I. INTRODUCTION.

Quantum phase transitions (QPTs)¹, the continuous phase transitions at zero temperature due to competing quantum ground states or quantum fluctuations, in correlated electron systems are of great fundamental importance and have been intensively studied over the past decades. Very recently, nano-systems (in particular quantum dots) offer an excellent playground to study QPTs due to high tunability²⁻⁷. The well-known Kondo effect^{8,9} plays a crucial role in understanding low energy properties in quantum dot devices. More interestingly, potential new QPTs in these systems may be realized in connection to exotic Kondo ground states. An outstanding example of an exotic Kondo state is the two-channel Kondo (2CK) system¹⁰, which has attracted much attention both theoretically and experimentally as it shows non-Fermi liquid behaviors at low temperatures. Experimentally, the 2CK behaviors have been realized in Ref.¹¹ where a quantum dot independently couples to an infinite and a finite reservoirs of non-interacting conduction electrons. More interestingly, the 2CK physics has also been found theoretically in Kondo quantum dot coupled to two strongly interacting Luttinger liquid leads with Luttinger parameter $K < 1/2$ ^{12,13}. An exotic quantum phase transition between the conducting 1CK phase for $K > 1/2$ and the insulating 2CK behaviors for $K < 1/2$ is expected to occur at $K = 1/2$ ¹². However, the critical properties of this 1CK-2CK QPT has not yet been addressed theoretically since it is not accessible to any controlled theoretical approaches.

On the other hand, a new type of materials—topological insulators (TIs)—with a gaped bulk and gapless edge states have been proposed theoretically¹⁴ and realized experimentally¹⁵. In 2D TIs, the gapless edge states have “helical” nature, *i.e.* the directions of spin and momen-

tum are locked together²⁶. The 2CK behaviors were argued to be stabilized in Kondo quantum dot coupled to two interacting helical edge states of 2D TIs for as long as $K < 1$ ¹⁶ based on bosonization and a simple scaling dimension analysis. In this paper, we re-examine the system in Ref.¹⁶ near 2CK fixed point via a controlled 1-loop renormalization group (RG) approach, which is beyond scaling dimension analysis. For a weak but finite lead-dot tunneling, we find that for $K < 1$ the 2CK fixed point can be unstable towards the 1CK fixed point and the system may undergo a quantum phase transition (QPT) between 1CK and 2CK fixed points. The QPT in our model comes as a result of the combined Kondo and the helical Luttinger physics in 2DTIs. It serves as the first example of the 1CK-2CK QPT that is accessible by the controlled perturbative RG approach. We extract the non-Fermi liquid behaviors from various thermodynamical quantities at the 1CK-2CK quantum critical point.

This paper is organized as follows. Sec. II will introduce the model Hamiltonian and its bosonized form as shown in Ref.¹⁶. In Sec. III we will present the RG analysis of the model both in the weak coupling limit (see Appendix A for details) and in the strong coupling limit near the 2CK fixed point (see Appendix B for details) via bosonization and re-fermionization of the model Hamiltonian. We will show that the RG analysis in both limits suggest a quantum phase transition between 1CK and 2CK fixed points. In Sec. IV we calculate via field-theoretical ϵ -expansion approach the critical properties and crossover functions of various thermodynamical observables. In Sec. V and Appendix C we perform stability analysis on the 1CK and 2CK fixed points respectively. We show that both fixed points are indeed stable fixed points, which substantiates our main finding that there exists an unstable quantum critical points separating two stable 1CK and 2CK fixed points.

II. MODEL HAMILTONIAN.

In our set-up, the Kondo Hamiltonian is given by¹⁶:

$$\begin{aligned}
H &= H_0 + H_K + H_{int} \\
H_0 &= -iv_F \sum_{i=1,2} \int_{-\infty}^{\infty} dx [c_{i,R}^{\dagger\uparrow}(x) \partial_x c_{i,R}^{\uparrow}(x) \\
&\quad - c_{i,L}^{\dagger\downarrow}(x) \partial_x c_{i,L}^{\downarrow}(x)] \\
H_K &= \sum_{i=1,2} J_1 \vec{S} \cdot \vec{s}_{i,i} + \sum_{i \neq j} J_2 \vec{S} \cdot \vec{s}_{i,j} \\
H_{int} &= \sum_{i,\sigma=\uparrow\downarrow} g_4 \int [c_{i,\alpha}^{\dagger\sigma}(x) c_{i,\alpha}^{\sigma}(x)]^2 dx \\
&\quad + g_2 \int c_{i,R}^{\dagger\uparrow}(x) c_{i,R}^{\uparrow}(x) c_{i,L}^{\dagger\downarrow}(x) c_{i,L}^{\downarrow}(x) dx \quad (1)
\end{aligned}$$

Here, H_0 describes the two-left (L) and right (R) conduction electron baths, H_K is the Kondo interaction, and the electron-electron interactions are given by H_{int} with $i = 1, 2, \alpha = R, L$. The conduction electron spin operator is given by: $\vec{s}_{i,j} = \sum_{k,k',\gamma,\delta} c_{ki}^{\dagger\gamma} \cdot \frac{\sigma_{\gamma\delta}}{2} \cdot c_{k'j}^{\delta}$ with $\gamma, \delta = \uparrow, \downarrow$. Note that in the presence of spin-orbit coupling, the spins \uparrow/\downarrow of the helical edge state electrons are locked with their right-moving (R)/left-moving (L) momentum. Note also that the small spin-orbit coupling will break the SU(2) spin-rotational symmetry in the above isotropic Kondo model, leading to the anisotropic Kondo model with $J_i^{xy} \neq J_i^z$ ¹⁶.

The Hamiltonian Eq. 1 can be bosonized through the standard Abelian bosonization¹⁹ for the electron operator^{16,21}: $c_{iR/L} = \frac{1}{\sqrt{2\pi a}} e^{\pm i(\sqrt{4\pi}\phi_{iR/L}(x) + k_F x)}$; the bosonic fields $\phi_i(x) = \phi_{iL}(x) + \phi_{iR}(x)$, $\theta_i(x) = \phi_{iL}(x) - \phi_{iR}(x)$, and the symmetric and antisymmetric combinations of ϕ_i , θ_i are: $\phi_{s/a} = \frac{1}{\sqrt{2}}(\phi_1 \pm \phi_2)$ and $\theta_{s/a} = \frac{1}{\sqrt{2}}(\theta_1 \pm \theta_2)$. Here we have dropped the spin indices of the edge state electrons due to their helical nature. The bosonized Hamiltonian is given by¹⁶:

$$\begin{aligned}
H &= H_0 - \sqrt{\frac{2}{\pi}} J_1^z S_z \partial_x \theta_s(0) \\
&\quad + J_2^z S_z \sin(\sqrt{\frac{2\pi}{K}} \theta_a(0)) \sin(\sqrt{2\pi K} \phi_a(0)) \\
&\quad + J_1^{xy} [S^- \exp^{-i(\sqrt{2\pi K} \phi_s(0))} + h.c.] \cos(\sqrt{2\pi K} \phi_a(0)) \\
&\quad + J_2^{xy} [S^- \exp^{-i(\sqrt{2\pi K} \phi_s(0))} + h.c.] \cos(\sqrt{\frac{2\pi}{K}} \theta_a(0)), \\
H_0 &= \frac{v'_F}{2} \int dx (\partial_x \phi_s)^2 + (\partial_x \theta_s)^2 + (\partial_x \phi_a)^2 + (\partial_x \theta_a)^2. \quad (2)
\end{aligned}$$

with $K = \sqrt{\frac{1+g_4/2\pi v_F - g_2/2\pi v_F}{1+g_4/2\pi v_F + g_2/2\pi v_F}}$ being the Luttinger parameter, $v'_F = v_F \sqrt{(1+g_4/2\pi v_F)^2 - (g_2/2\pi v_F)^2}$.

III. RG ANALYSIS OF THE MODEL.

A. RG analysis in weak coupling fixed point: $J_i^{xy,z} = 0$

In the vicinity of the fixed point $J_i^{xy,z} = 0$, it has been shown in Ref.¹⁶ that the scaling dimensions of these Kondo couplings based on the bosonized Hamiltonian Eq. 1 of Ref.¹⁶ are: $[J_1^{xy}] = K < 1$, $[J_1^z] = 1$, $[J_2^{xy}] = [J_2^z] = 1/2(K+1/K) > 1$ where $K < 1$ for repulsive electron interactions. The authors of Ref.¹⁶ argued that for $K < 1$, under renormalization group (RG) transformations, the 2CK fixed point is reached as the relevant J_1 couplings flow to large values with decreasing temperatures; while the irrelevant J_2 couplings decrease to zero. However, we find for $K \rightarrow 1^-$ that all four Kondo couplings can flow to large values, depending on the values of K and the values of the bare Kondo couplings. This suggests a stable 1CK fixed point in the parameter space of the model.

To derive the 1-loop RG scaling equations, we first re-fermionize Eq. 2 to arrive an effective Kondo model:

$$\begin{aligned}
H_{eff} &= \tilde{H}_0 + \tilde{H}_K \\
\tilde{H}_0 &= \sum_{k,\alpha,\beta=L,R,\sigma=\uparrow,\downarrow} \epsilon(k) \tilde{c}_{k\alpha}^{\dagger\sigma} \tilde{c}_{k\beta}^{\sigma}, \\
\tilde{H}_K &= J_1^{xy} [e^{-i(\sqrt{4\pi K} - \sqrt{4\pi})\phi_1} s_{LL}^+ \\
&\quad + e^{i(\sqrt{4\pi K} - \sqrt{4\pi})\phi_2} s_{RR}^+] S^- + h.c. \\
&\quad + J_1^z (s_{LL}^z + s_{RR}^z) S_z \\
&\quad + J_2^{xy} S^- [e^{i(\sqrt{\pi K} - \sqrt{\pi})\phi_1 + i(\sqrt{\pi/K} - \sqrt{\pi})\theta_1} \\
&\quad \times e^{i(\sqrt{\pi K} - \sqrt{\pi})\phi_2 - i(\sqrt{\pi/K} - \sqrt{\pi})\theta_2} s_{LR}^+ \\
&\quad + e^{i(\sqrt{\pi K} - \sqrt{\pi})\phi_1 - i(\sqrt{\pi/K} - \sqrt{\pi})\theta_1} \\
&\quad \times e^{i(\sqrt{\pi K} - \sqrt{\pi})\phi_2 + i(\sqrt{\pi/K} - \sqrt{\pi})\theta_2} s_{RL}^+] + h.c. \\
&\quad + J_2^z S_z [e^{-i(\sqrt{\pi K} - \sqrt{\pi})\phi_1 - i(\sqrt{\pi K} - \sqrt{\pi})\phi_2} \\
&\quad \times e^{i(\sqrt{\pi/K} - \sqrt{\pi})\theta_1 - i(\sqrt{\pi/K} - \sqrt{\pi})\theta_2} \sum_{k,k'} \tilde{c}_{kL}^{\dagger\uparrow} \tilde{c}_{k'R}^{\uparrow} \\
&\quad - e^{i(\sqrt{\pi K} - \sqrt{\pi})\phi_1 + i(\sqrt{\pi K} - \sqrt{\pi})\phi_2} \\
&\quad \times e^{i(\sqrt{\pi/K} - \sqrt{\pi})\theta_1 - i(\sqrt{\pi/K} - \sqrt{\pi})\theta_2} \sum_{k,k'} \tilde{c}_{kL}^{\dagger\downarrow} \tilde{c}_{k'R}^{\downarrow}] \\
&\quad + h.c.. \quad (3)
\end{aligned}$$

Here, \tilde{H}_0 describes the effective non-interacting fermion leads with $\tilde{c}_{\alpha\sigma}$ being the electron destruction operator of the effective non-interacting lead α , $s_{\gamma\beta}^{\pm(z)} = \sum_{\alpha,\delta,k,k'} 1/2 \tilde{c}_{k\gamma}^{\dagger\alpha} \sigma_{\alpha\delta}^{\pm(z)} \tilde{c}_{k'\beta}^{\delta}$ are the spin-flip (z-component of the spin) operators between the effective leads γ and β , and \tilde{H}_K being the effective Kondo coupling terms. Note that the Kondo couplings in Eq. 3 acquire additional phase factors coming from the interactions in the original leads via bosonization. These phases lead

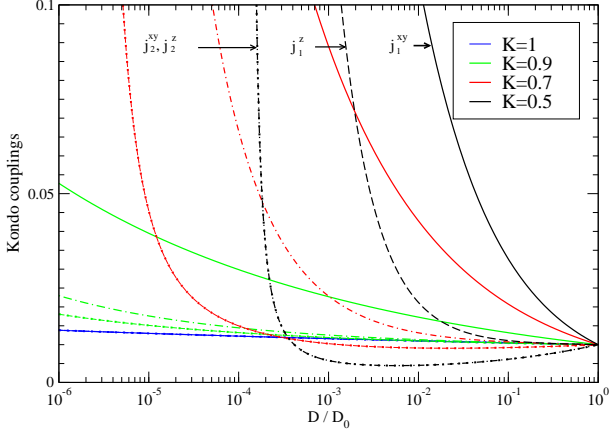


FIG. 1: (Color online) RG flows of various Kondo couplings in the weak-coupling regime with fixed bare Kondo couplings: $j_i^{xy,z} = 0.01D_0$ and $D_0 = 1$. Curves with different colors indicate the RG flows with different Luttinger parameters K .

to the non-trivial bare scaling dimensions and therefore to the first term (linear in the Kondo coupling) of the RG scaling equations. Following the similar steps via poor-man's scaling technique as shown in Ref.²² for a dissipative Kondo dot, the 1-loop RG scaling equations near $J_i^{xy,z} = 0$ are hence given by (see Appendix A. for details):

$$\begin{aligned} \frac{\partial j_1^{xy}}{\partial \ln D} &= (K-1)j_1^{xy} - j_1^{xy}j_1^z - j_2^{xy}j_2^z, \\ \frac{\partial j_1^z}{\partial \ln D} &= -(j_2^{xy})^2 - (j_1^{xy})^2, \\ \frac{\partial j_2^{xy}}{\partial \ln D} &= [1/2(K+1/K) - 1]j_2^{xy} - j_2^{xy}j_1^z - j_1^{xy}j_2^z, \\ \frac{\partial j_2^z}{\partial \ln D} &= [1/2(K+1/K) - 1]j_2^z - 2j_1^{xy}j_2^{xy}. \end{aligned} \quad (4)$$

where the dimensionless Kondo couplings are defined as: $j_1^{xy} = \mu^{K-1}J_1^{xy}$, $j_1^z = J_1^z$, $j_2^{xy} = \mu^{1/(K+1/K)-1}J_2^{xy}$, and $j_2^z = \mu^{1/(K+1/K)-1}J_2^z$ with μ being an energy scale. Note that the linear term in the above RG scaling equations come from the non-trivial scaling dimensions of the corresponding Kondo couplings; while the quadratic terms in Kondo couplings are the corrections at 1-loop order. For $K \rightarrow 1^-$, both $J_z^{xy,z}$ terms are marginally irrelevant, $[J_2^{xy,z}] \rightarrow 1^-$. Therefore, within the validity of perturbative RG, both $J_2^{xy,z}$ terms can still flow to a large value if bare Kondo couplings $J_i^{xy,z}$ are large enough (but they are still in order of $1-K \ll 1$), leading to (possibly) 1CK fixed point (ie., the quadratic terms overcome the linear term in RG equations). However, for small enough bare Kondo couplings, $J_2^{xy,z}$ terms are irrelevant and hence the system moves towards the 2CK fixed point. As shown in Fig. 2, in the relatively higher temperature (energy) regime $10^{-3} < D/D_0 < 1$,

with decreasing K the system tends to flow to 2CK fixed point where $J_1^{xy,z}$ flow to large values while $J_2^{xy,z}$ decreases with decreasing temperature (energy). It is therefore reasonable to expect a 1CK-2CK quantum phase transition in the 4-dimensional parameter space of $J_{1,2}^{xy,z}$. However, the above weak coupling RG analysis breaks down at a low enough temperature (energy) when the system gets closer to the strong coupling regime, which explains the increase of $J_2^{xy,z}$ in Fig. 2 at lower temperatures for smaller K . Therefore, to address the possible quantum phase transition between 1CK and 2CK fixed points, it is necessary to be able to access the neighborhood of the strong-coupling 2CK fixed point as we shall discuss below.

B. RG analysis near strong coupling (2CK) fixed point

The authors in Ref.¹⁶ did scaling dimension analysis near a strong coupling regime where $J_1^z = \mathcal{O}(1)$, $J_2^{xy,z} = J_1^{xy} = 0$. They performed the Emery-Kivelson unitary transformation to the bosonized Hamiltonian (Eq. 1 of Ref.¹⁶), and arrived Eq. 2 of Ref.¹⁶.

$$\begin{aligned} H &= H_0 - \tilde{J}_1^z S_z \partial_x \theta_s(0) \\ &+ J_2^z S_z \sin\left(\sqrt{\frac{2\pi}{K}}\theta_a(0)\right) \sin\left(\sqrt{2\pi K}\phi_a(0)\right) \\ &+ (S^- + S^+)[J_1^{xy} \cos(\sqrt{2\pi K}\phi_a(0)) \\ &+ J_2^{xy} \cos\left(\sqrt{\frac{2\pi}{K}}\theta_a(0)\right)] \end{aligned} \quad (5)$$

with $-\tilde{J}_1^z = \sqrt{2\pi K}v_F - \sqrt{\frac{2}{\pi K}}J_1^z$.

They found the scaling dimensions for the Kondo couplings to be $[J_1^{xy}] = K/2$, $[J_2^{xy}] = 1/(2K)$, $[J_2^z] = 1/2(K+1/K)$. The J_1^{xy} term is relevant for $K < 1$, and J_2^{xy} term is relevant for $1/2 < K < 1$. As $K \rightarrow 1^-$, J_2^z becomes marginally irrelevant, and it can flow to a large value under RG if the bare Kondo couplings are large enough once the 1-loop RG is performed. This seems to suggest a stable 1CK near strong coupling regime as all of the four Kondo couplings can either flow to or stay at large values (of order 1).

To gain more insight into the stability of the 1CK/2CK fixed point, we apply RG approach at 1-loop order together with bosonization and re-fermionization near 2CK fixed point. We first map the bosonized Hamiltonian Eq. 1 of Ref.¹⁶ onto an effective Kondo model via re-fermionization: Near the strong coupling 2CK fixed point $J_1^{xy} \rightarrow \infty$, $J_2^z \rightarrow 0$, $J_2^{xy} \rightarrow 0$, the effective Hamiltonian reads¹⁶: $H_{2CK} = H_0 + \frac{2J_2^{xy}}{\pi a} S_x \cos(\sqrt{2\pi K}\phi_a(0))$. Note that near 2CK fixed point, S_x commutes with H_{2CK} , we may therefore set S_x to its eigenvalue $\pm 1/2$ in H_{2CK} . The the scaling dimensions of Kondo couplings near 2CK

fixed point are¹⁶ $[J_2^{xy}] = \frac{1}{K}$, $[\tilde{J}_1^z] = 1 + \frac{1}{2K}$, $[J_2^z] = \frac{1}{K} + \frac{K}{2}$. Note that all the above three couplings are irrelevant for $K < 1$. This suggests that the 2CK fixed point is a stable fixed point for $K < 1$.

Meanwhile, by a stability analysis near the strong coupling 1CK fixed point (see Sec. V.), we are able to show that the 1CK fixed point is also a stable one for $K < 1$. Since both 1CK and 2CK fixed points are stable in their neighborhood, this opens up a possibility of the existence of a quantum phase transition (and an unstable critical fixed point) between 1CK and 2CK fixed points of the model.

To address this issue, we shall focus below on the RG flows of the leading two irrelevant operators near the 2CK fixed point, given by:

$$\delta H_{2CK} = J_2^{xy} S^x \cos\left(\sqrt{\frac{2\pi}{K}}\theta_a(0)\right) - \tilde{J}_1^z S_z \partial_x \theta_s(0). \quad (6)$$

Via re-fermionization, we can map $H_0 + \delta H_{2CK}$ onto an effective Kondo model subject to a bosonic environment:

$$\begin{aligned} H_0 + \delta H_{2CK} = & \sum_{k,\sigma,i=L,R} \epsilon(k) \tilde{c}_{k,i\sigma}^\dagger \tilde{c}_{k,i\sigma} + \epsilon v_F \int dx (\partial_x \tilde{\theta})^2 \\ & + J_2^{xy} S^- [s_{LR}^+ e^{i\sqrt{4\pi(\frac{1}{K}-1)}\tilde{\theta}(0)} \\ & + s_{RL}^+ e^{-i\sqrt{4\pi(\frac{1}{K}-1)}\tilde{\theta}(0)}] \\ & + J_2^{xy} S^+ [s_{LR}^- e^{-i\sqrt{4\pi(\frac{1}{K}-1)}\tilde{\theta}(0)} \\ & + s_{RL}^- e^{i\sqrt{4\pi(\frac{1}{K}-1)}\tilde{\theta}(0)}] \\ & + \tilde{J}_1^z (s_{LL}^z + s_{RR}^z) S_z \end{aligned} \quad (7)$$

where the effective bosonic field $\tilde{\theta}(0)$ is defined through $\frac{\theta_a}{\sqrt{K}} = \sqrt{2}\theta_0 + \sqrt{\frac{2}{K}-2}\tilde{\theta}$, $\frac{\theta_s}{\sqrt{K}} = \sqrt{2}\theta_0 - \sqrt{\frac{2}{K}-2}\tilde{\theta}$, and we have omitted the $\phi_{s/a}$ fields in H_0 as they do not couple to δH_{2CK} . Here, $s_{\alpha\beta}^{\pm,z}$ refers to the spin operators between the effective non-interacting leads α and β as defined previously. Via re-fermionization the effective conduction electron operator is defined as: $\tilde{c}_{L(R)}^{\uparrow(\downarrow)} = F_{L(R)} e^{i\phi_1^{\uparrow(\downarrow)}}$ with $F_{L(R)}$ being the Klein factors, and $\sqrt{2}\theta_0 \equiv \phi_1^\uparrow - \phi_2^\downarrow$. Note that the bosonic field $\tilde{\theta}$ obeys the following correlation: $\langle e^{-i\sqrt{4\pi(\frac{1}{K}-1)}\tilde{\theta}(t)} e^{i\sqrt{4\pi(\frac{1}{K}-1)}\tilde{\theta}(0)} \rangle \propto \frac{1}{t^{2(\frac{1}{K}-1)}}$; while the impurity spin operator S_z exhibits the following correlation: $\langle S_z(t) S_z(0) \rangle \propto \frac{1}{t^{1/K}}$ ¹⁶.

To obtain the one-loop RG scaling equations for J_2^{xy} and \tilde{J}_1^z in Eq. 7, we define the dimensionless couplings $j_2^{xy} \equiv \mu^\epsilon J_2^{xy}$ and $j_1^z \equiv \mu^{\epsilon'} \tilde{J}_1^z$ and $\epsilon \equiv \frac{1}{K} - 1$, $\epsilon' \equiv \frac{1}{2K}$. Via a similar poor-man's scaling approach²² that leads to Eq. 4 in the weak coupling regime, we find (see Appendix

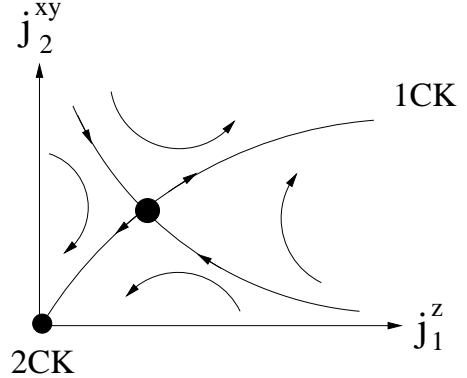


FIG. 2: (Color online) Schematic diagram of the RG flow near 2CK fixed point. The 1CK-2CK quantum critical point is represented by the filled black circle located at $j_c = (j_2^{xy}, j_1^z) = (\sqrt{\epsilon\epsilon'}, \epsilon)$.

A.):

$$\begin{aligned} \frac{\partial j_2^{xy}}{\partial \ln D} &= \epsilon j_2^{xy} - j_2^{xy} j_1^z, \\ \frac{\partial j_1^z}{\partial \ln D} &= \epsilon' j_1^z - (j_2^{xy})^2. \end{aligned} \quad (8)$$

For $K \rightarrow 1^-$ we find an intermediate quantum critical point (QCP) at $j_c = (j_2^{xy}, j_1^z)$ within the validity of the perturbative RG separating the stable 1CK and 2CK fixed points where $j_2^{xy} = \sqrt{\epsilon\epsilon'}$, $j_1^z = \epsilon$. The RG flows near the QCP are determined by linearizing the RG scaling equations as shown in Fig. 2. Meanwhile, as the initial couplings (j_2^{xy}, j_1^z) lie on the upper-right corner of the phase diagram in Fig. 2, the 2CK fixed point is unstable and both couplings will flow to a fixed point with large values. We will show that this fixed point is the familiar 1CK fixed point where all the four Kondo couplings will flow to (or stay at) large values. First, j_1^z is already taken to be a large value in our strong coupling RG analysis. Since in this parameter regime both j_1^z and j_2^{xy} will also flow to large values, we shall look at the RG flow of the remaining most irrelevant coupling j_2^{xy} :

$$\frac{\partial j_2^{xy}}{\partial \ln D} = \left[\frac{1}{K} + \frac{K}{2} - 1 \right] j_2^{xy} - j_1^z j_2^{xy} \quad (9)$$

where the dimensionless couplings are defined as: $j_1^z = \mu^{K/2-1} J_1^z$, $j_2^{xy} = \mu^{1/K+K/2-1} J_2^{xy}$. It is clear from Eq. 9 that if j_2^{xy} becomes relevant (flows to a large value under RG), j_2^{xy} will also become relevant eventually though it is irrelevant at the tree-level based on the bare scaling dimensional analysis in Ref.¹⁶.

IV. CRITICAL PROPERTIES NEAR 1CK-2CK QUANTUM PHASE TRANSITION.

The critical properties and crossovers of various thermodynamical quantities near the 1CK-2CK QCP can be

obtained via the above RG approach combined with the field-theoretical ϵ -expansion technique^{23,25}. We employ here a double- ϵ -expansion with two small expansion parameters ϵ and ϵ' . Our approach is valid for the Luttinger parameter $K \rightarrow 1$ as both parameters ϵ and ϵ' are small: $\epsilon \rightarrow 0$, $\epsilon' \rightarrow 1/2 < 1$. Following Refs.^{23,25}, we define the renormalized fields \tilde{f}_σ and dimensionless Kondo couplings j as: $f_\sigma = \sqrt{Z_f} \tilde{f}_\sigma$, and $J_2^{xy} = \frac{\mu^{-\epsilon} Z_{j^\perp}}{Z_f} j_2^{xy}$, $\tilde{J}_1^z = \frac{\mu^{-\epsilon'} Z_{j^z}}{Z_f} j_1^z$ with Z_f and $Z_{j^\perp/z}$ being the renormalization factors for the impurity field and Kondo couplings, respectively and μ is a renormalization energy scale. The renormalization factors are obtained via minimal subtractions of poles^{23,25}, given by (see Appendix B.):

$$\begin{aligned} Z_{j^\perp} &= 1 + \frac{j_1^z}{\epsilon'} \\ , Z_{j^z} &= 1 + \frac{(j_2^{xy})^2 / j_1^z}{2\epsilon} \\ Z_f &= 1 + \frac{(j_2^{xy})^2}{8\epsilon} + \frac{(j_1^z)^2}{16\epsilon'}. \end{aligned} \quad (10)$$

Within the field-theoretical RG approach, we have checked that the RG scaling equations in Eq. 8 can be reproduced via calculating the β -functions: $\beta(j_i) \equiv \mu \frac{\partial j_i}{\partial \mu}|_{j_i}$ with μ being an energy scale, $j_i = j_2^{xy}, j_1^z$ and $J_i = J_2^{xy}, J_1^z$ (see Appendix B.). Below we discuss various critical properties and crossover functions based on field-theoretical ϵ -expansion approach.

A. Observables at criticality

We first calculate various observables at criticality, including correlation length exponent, impurity entropy, dynamical properties of the T-matrix and local spin susceptibility.

1. Correlation length exponent ν

The correlation length exponent ν describes the power-law behavior of the characteristic crossover energy scale T^* when the system is tuned to the transition: $T^* \propto |t|^\nu$ with $t \equiv \frac{j-j_c}{j_c}$ being the dimensionless distance to the QCP and $j \equiv (j_2^{xy}, j_1^z)$. To calculate ν , we may first linearize the RG scaling equations Eq.8 near QCP. The correlation length exponent ν is determined by the largest eigenvalue of the coupled linearized equations, found to be:

$$\nu = \frac{1}{2\epsilon}. \quad (11)$$

2. Impurity entropy

The impurity contribution to the low-temperature entropy near QCP is obtained by a perturbative calculation of the impurity thermodynamic potential Ω_{imp} ²³ with respect to the 2CK fixed point and taking the temperature derivative: $S_{imp} = \frac{\partial \Omega_{imp}}{\partial T}$. At QCP and $T = 0$ it can be written as:

$$S_{imp}^{QCP} = S_{imp}^{2CK} + \Delta S_{imp}. \quad (12)$$

where $S_{imp}^{2CK} = \ln \sqrt{2K} = \frac{1}{2} \ln 2K$ is the zero-temperature residual impurity entropy at 2CK fixed point which shows the existence of fractionally degenerate ground state¹⁶⁻¹⁸, and ΔS_{imp} is the correction to S_{imp}^{2CK} at QCP. Following similar renormalized perturbative calculations in Ref.²³, we find

$$\Delta S_{imp} = \pi^2 \ln 2 \left[\frac{\epsilon (j_{2c}^{xy})^2}{4} + \frac{\epsilon' (j_{1c}^z)^2}{8} \right] = \frac{3\epsilon^2 \pi^2 \ln 2}{16K}. \quad (13)$$

3. The T-matrix

The conduction electron T -matrix, $T(\omega)_{\alpha\alpha'}$, in the Kondo model carries important information on the scattering of the conduction electrons from lead α to lead α' via the impurity. In particular, $T_{\alpha\alpha'}(\omega)$ with $\alpha \neq \alpha'$ describes the transport across the dot, detectable in transport measurements. The T -matrix is determined from the conduction electron Green functions $G_{\alpha\alpha'}(t) = \langle c_\alpha(0) c_{\alpha'}^\dagger(t) \rangle$ through $G_{\alpha\alpha'} = G_{\alpha\alpha'}^0 \delta_{\alpha\alpha'} + G_{\alpha\alpha}^0(\omega) \delta_{\alpha\alpha'} T_{\alpha\alpha'}(\omega) G_{\alpha'\alpha'}^0(\omega)$. At the 2CK fixed point, we find $Im(T_{\alpha\alpha'}(\omega)) \propto \frac{1}{\omega^{-\eta_T^{2CK}}}$ with $\alpha \neq \alpha'$ the anomalous power-law exponent at the tree-level being $\eta_T^{2CK} = \epsilon$. Near 1CK-2CK QCP, however, $Im(T_{\alpha\alpha'}(\omega))$ acquires an additional anomalous power-law behavior:

$$Im(T_{\alpha\alpha'}(\omega)) \propto \frac{1}{\omega^{-\eta_T^{2CK} - \Delta\eta_T}}. \quad (14)$$

where the anomalous exponent $\Delta\eta_T$ is obtained via the renormalization factor Z_T for the T -matrix propagator $T_{\alpha\alpha'}(\omega)$: $\Delta\eta_T = \beta(j_2^{xy}) \frac{\partial \ln Z_T}{\partial j_2^{xy}}|_{j_2^{xy}}$. Here, the renormalization factor Z_T is obtained by minimal subtraction of poles^{23,25}: $Z_T = \frac{Z_f^2}{Z_{j^\perp}^2}$. We find therefore

$$\Delta\eta_T = \frac{(J_{2c}^{xy})^2}{2} = \frac{\epsilon}{4K}. \quad (15)$$

4. Local spin susceptibility $Im(\chi_{zz}(\omega))$

The imaginary part of the local dynamical spin susceptibility $Im(\chi_{zz}(\omega))$ is defined as the time Fourier transform of the correlator: $\langle S_z(0) S_z(t) \rangle$. It shows a power-law behavior at QCP:

$$Im(\chi(\omega)_{QCP}) \propto \frac{1}{\omega^{1-\eta_\chi^{2CK} - \Delta\eta_\chi}}. \quad (16)$$

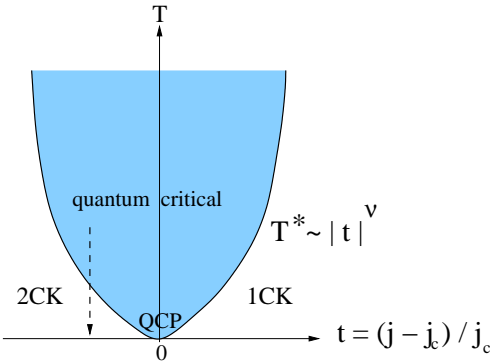


FIG. 3: (Color online) Schematic finite temperature phase diagram of our model near 1CK-2CK quantum critical point. As $T \rightarrow 0$, the 1CK ground state is reached when $t > 0$ or $j > j_c$; while as the 2CK ground state is reached for $t < 0$ or $j < j_c$. Here, $j > (<)j_c$ refers to the upper right (lower left) region in the phase diagram shown in Fig. 2. The dashed vertical arrow at $t < 0$ refers to the finite temperature crossover between the quantum critical region (blue shaded area bounded by the crossover temperature T^*) and the 2CK ground state, which is our interest. Here, j and j_c are defined in the text.

Here, $\eta_{\chi}^{2CK} = \frac{1}{K}$ is the anomalous exponent of $Im(\chi_{zz}(\omega))$ at 2CK fixed point via the power-law behavior of the correlator $\langle S_z(0)S_z(t) \rangle$ evaluated at 2CK fixed point¹⁶, and $\Delta\eta_{\chi}$ is the correction to the anomalous exponent at 2CK when the system is at QCP. Via ϵ -expansion within the field-theoretical RG framework^{23,25}, $\Delta\eta_{\chi}$ is obtained by: $\Delta\eta_{\chi} = \beta(j_2^{xy}) \frac{\partial \ln Z_{\chi}}{\partial j_2^{xy}}|_{j_2^{xy}, j_1^z} + \beta(j_1^z) \frac{\partial \ln Z_{\chi}}{\partial j_1^z}|_{j_2^{xy}, j_1^z}$ with $Z_{\chi} = Z_f^2$ being the renormalization factor for the impurity susceptibility. Carrying out the above calculations, finally we arrive at

$$\Delta\eta_{\chi} = \frac{(j_{2c}^{xy})^2}{2} + \frac{(j_{1c}^z)^2}{4} = \frac{\epsilon}{4K} + \frac{\epsilon^2}{4} \quad (17)$$

at QCP.

B. Crossover near critical point

Next, we calculate the crossover functions close to the 1CK-2CK quantum critical point. In particular, we may access the crossover behaviors between QCP and 2CK fixed points where our RG and ϵ -expansion approach is controlled (see Fig. 3). To simplify the calculations and obtain analytic results, we focus on the crossover along the curve where $\beta(j_1^z) = 0$, (or equivalently along the curve satisfying $j_1^z = 2K(j_2^{xy})^2$). Under this constraint, only one RG β -function ($\beta(j_2^{xy})$) remains:

$$\beta(j_2^{xy}) = \epsilon j_2^{xy} - 2K(j_2^{xy})^3. \quad (18)$$

The simple analytic solution for the above equation between QCP located at $j_{2c}^{xy} = \sqrt{\frac{\epsilon}{2K}}$ (the same value as

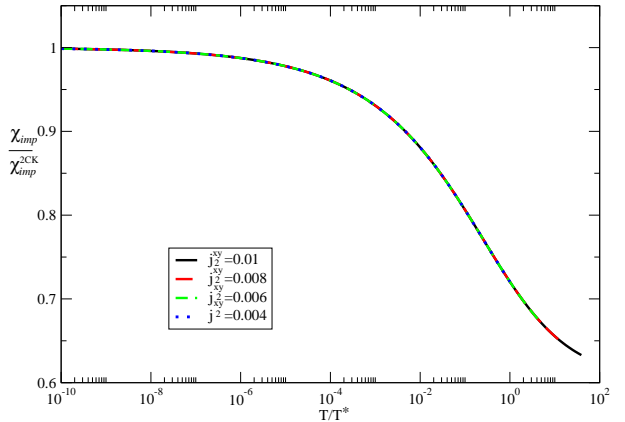


FIG. 4: (Color online) χ_{imp}/χ_{2CK} versus T/T^* (see Eq.20) at fixed $K = 0.8$ for various bare Kondo couplings where $j_1^z = 2K(j_2^{xy})^2$ is satisfied and $j_{2c}^{xy} = \sqrt{\frac{\epsilon}{2K}} \approx 0.39$.

$j_{2c}^{xy} = \sqrt{\epsilon\epsilon'}$ obtained in Sec. III B) and 2CK fixed points ($j_2^{xy} < j_{2c}^{xy}$) is found to be:

$$j_2^{xy}(D) = \frac{j_{2c}^{xy}}{\sqrt{1 + (\frac{D}{T^*})^{-2\epsilon}}}. \quad (19)$$

where $T^* = (\frac{(j_{2c}^{xy})^2 - (j_2^{xy})^2}{(j_2^{xy})^2})^{\frac{1}{2\epsilon}}$ is the crossover energy scale. Eq. 19 can be used to compute various crossovers in thermodynamic functions near 1CK-2CK QCP as discussed below.

1. The impurity susceptibility $T\chi_{imp}$

The impurity susceptibility is defined as^{23,24}: $\chi_{imp}(T) = \chi_{imp,imp} + 2\chi_{u,imp} + (\chi_{u,u} - \chi_{u,u}^{bulk})$ where $\chi_{u,u}$ is the bulk response to the local field applied to the bulk only, $\chi_{imp,imp}$ is the impurity response to the local field applied to the impurity only, $\chi_{u,imp}$ is the crossed response of the bulk to an impurity field, $\chi_{u,u}^{bulk}$ is the susceptibility of the bulk in the absence of the impurity. We can calculate $\chi_{imp}(T)$ via perturbative approaches in Refs.^{23,24}. We find (up to the first order in j_2^{xy}) $\chi_{imp}(T)$ has the following crossover form (see Eq. 19 and Fig. 4):

$$\begin{aligned} \frac{\chi_{imp}(T)}{\chi_{2CK}^{2CK}(T)} &\approx 1 - j_2^{xy}(D \rightarrow T) \\ &= 1 - \frac{j_{2c}^{xy}}{\sqrt{1 + (\frac{T}{T^*})^{-2\epsilon}}} \end{aligned} \quad (20)$$

where χ_{imp}^{2CK} is the impurity susceptibility at the 2CK fixed point, given by $\chi_{imp}^{2CK}(T) = \frac{1}{4} \frac{1}{T^{1-\eta_{\chi}^{2CK}}}$ with $\eta_{\chi}^{2CK} = \frac{1}{K}$.

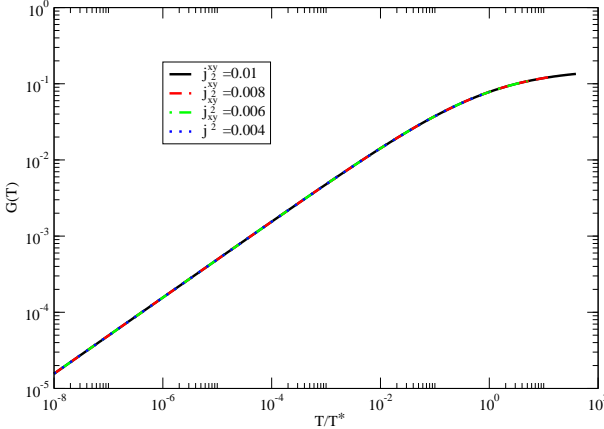


FIG. 5: (Color online) Crossover of the linear conductance $G(T)$ versus T/T^* (see Eq.22) at fixed $K = 0.8$ for various bare Kondo couplings (same as in Fig.4).

2. Impurity entropy S_{imp}

At 2CK fixed point, the impurity residual entropy has been calculated in Ref.¹⁶: $S_{imp}^{2CK} = \ln \sqrt{2K}$. Following Ref.²³, the correction to S_{imp}^{2CK} near QCP is obtained within perturbative RG approach by calculating the thermodynamic potential and taking the temperature derivative. The crossover function for the impurity entropy near QCP is found to be²³:

$$\begin{aligned} \frac{S_{imp}(T)}{S_{imp}^{2CK}} &\approx 1 + \frac{\pi^2 \epsilon}{4} \frac{\ln 2}{\ln \sqrt{2K}} [j_2^{xy}(D \rightarrow T)]^2 \\ &= 1 + \frac{\pi^2 \epsilon}{4} \frac{\ln 2}{\ln \sqrt{2K}} \left[\frac{j_{2c}^{xy}}{\sqrt{1 + (\frac{T}{T^*})^{-2\epsilon}}} \right]^2. \end{aligned} \quad (21)$$

3. Equilibrium conductance $G(T)$

The equilibrium conductance $G(T)$ has the following crossover form between 2CK fixed point and the QCP (see Fig. 5):

$$G(T) = [j_2^{xy}(D \rightarrow T)]^2 = \frac{[j_{2c}^{xy}]^2 T^{2\epsilon}}{T^{2\epsilon} + (T^*)^{2\epsilon}}. \quad (22)$$

Note that in equilibrium the linear conductance at 2CK fixed point $G_{2CK}(T)$ is determined by the bare scaling dimension of the leading irrelevant operator j_2^{xy} , $[j_2^{xy}] = \epsilon$. This gives $G_{2CK}(T) \propto T^{2[j_2^{xy}]} = T^{2\epsilon}$. For $T \ll T^*$ where the system reaches the 2CK fixed point, the temperature dependence of $G(T)$ in Eq. 22 reduces to that at 2CK, $G(T) \rightarrow G_{2CK}(T)$, as expected.

V. STABILITY ANALYSIS OF 1CK FIXED POINT FOR $K < 1$.

We furthermore show the stability of this 1CK fixed point for $K \leq 1$. Following Eq. 2 of Ref.¹⁶, the Hamil-

tonian in the bosonized form is given by:

$$\begin{aligned} H_K &= -\tilde{J}_1^z S_z \partial_x \theta_s \\ &+ J_2^z S_z \sin\left(\sqrt{\frac{2\pi}{K}} \theta_a\right) \sin(\sqrt{2\pi K} \phi_a) \\ &+ J_1^{xy} S_x \cos(\sqrt{2\pi K} \phi_a) \\ &+ J_2^{xy} S_x \cos\left(\sqrt{\frac{2\pi}{K}} \theta_a\right). \end{aligned} \quad (23)$$

Here, we keep all the four Kondo couplings near 1CK fixed point as they will all flow to large values. At 1CK fixed point, conduction electrons on both leads at $x = \pm a$ (the closest location to the quantum dot) form the Kondo spin-singlet with impurity (quantum dot) spin located at $x = 0$. The effective Hamiltonian near 1CK fixed point may take the following form⁸:

$$\begin{aligned} \delta H_{1CK} &\approx H_t + H_u, \\ H_t &= t \sum_{j=R,L} c_{e,j\sigma}^\dagger(2a) c_{e,j\sigma}(a), \\ H_u &= u(c_{e\sigma}^\dagger(a) c_{e\sigma}(a) - 1)^2 \end{aligned} \quad (24)$$

where $c_{e,\sigma}$ is the even combination of the electron destruction operator in leads 1 and 2, a represents the lattice constant and $x = a$ is the nearest-neighbor site to $x = 0$. (Note that in the 1-channel Kondo limit, only the even combination of the conduction electrons in the two leads will contribute to the formation of the Kondo singlet.) Here, H_t describes the hopping of electrons between $x = a$ and $x = 2a$. (Note that δH_{1CK} does not involve conduction electrons at site $x = 0$ since they form Kondo singlet with the impurity spin.) Upon bosonizing H_t , one can show that it just renormalizes the kinetic term H_0 . The H_u term with $u > 0$ is the on-site electron-electron interaction at $x = a$; it contains two-particle forward and Umklapp scattering terms. The forward scattering terms just renormalize the g_2 and g_4 terms mentioned above. The Umklapp term (H_{um}) takes the following form^{16,26}:

$$H_{um} = g_u e^{4ik_f a} (\psi_R^\dagger(0) \psi_R^\dagger(0) \psi_L(0) \psi_L(0)) + h.c. \quad (25)$$

with $\psi_{R(L)\uparrow(\downarrow)} \equiv c_{e,R(L)\uparrow(\downarrow)}$. Only the Umklapp term has the potential to open up a gap at the filling $k_f = \frac{\pi}{2a}$.²⁶ Via bosonization: $\psi_{R(L)} = \frac{1}{\sqrt{2\pi a}} e^{\pm i(\sqrt{4\pi} \phi_{R(L)\uparrow(\downarrow)}(x) + k_F x)}$, we have: $H_{um} \propto g_u \cos(\sqrt{32\pi/K} \theta)$ where we change our basis from $(\phi_L^\downarrow, \phi_R^\uparrow)$ to $(\theta \equiv \frac{\phi_L^\downarrow - \phi_R^\uparrow}{\sqrt{2}}, \phi \equiv \frac{\phi_L^\downarrow + \phi_R^\uparrow}{\sqrt{2}})$. The scaling dimension of g_u was found to be $8/K$, which is always irrelevant for $K \leq 1$ ^{16,26}.

Note that in general there exists the single particle backscattering term due to the interaction of $\psi_{R/L}(0)$ and the quantum dot¹⁶: $t' \psi_R^\dagger \psi_L + h.c.$. However, this term is forbidden here as it breaks time-reversal symmetry. Also note that for 1-D Hubbard model in general

there exists the “spin-flip” backscattering term in H_u of the form: $H_{sf} \propto \psi_L^{\dagger\uparrow} \psi_L^{\downarrow} \psi_R^{\dagger\downarrow} \psi_R^{\uparrow} + h.c.$. However, due to the helical nature of our leads (or the Right/Left moving electrons are tied to their spins, *i.e.* only $\psi_{R(L)}^{\uparrow(\downarrow)}$ electrons exist), this H_{sf} term is absent here.

From above, we conclude that 1CK fixed point is stable against small perturbations for $K \leq 1$. As a consistency check, in Appendix C, we generalize the above argument to address the stability of the 1CK and 2CK fixed points for a Kondo dot couples to two Luttinger liquid leads. We find that the 1CK fixed point is stable for $1/2 < K < 1$, and unstable for $K < 1/2$; while the 2CK fixed point is stable for $K < 1/2$, and unstable for $K > 1/2$, consistent with the known result¹².

VI. CONCLUSIONS.

Based on Ref.¹⁶, we have re-examined the 2-channel Kondo physics in the Kondo quantum dot coupled to two helical edge states of 2-dimensional topological insulators. Via the 1-loop renormalization group approach which goes beyond the scaling dimension analysis in Ref.¹⁶, we found the quantum phase transition between the 1-channel and 2-channel Kondo ground states for weakly interacting leads ($K \rightarrow 1^-$). We made definite predictions on the critical properties when the system is close to the transition. Our results refined the statement in Ref.¹⁶ that the 2-channel Kondo ground state is stable for as long as $K < 1$; they also provide the first theoretical realization of the quantum phase transition between 1CK and 2CK physics in Kondo impurity models. Our results also motivate the search for these critical properties near 1CK-2CK quantum phase transition in future experiments on Kondo quantum dot coupled to 2D topological insulators.

Acknowledgments

We thank M. Vojta, T.K. Ng, and K.T. Law for helpful discussions. This work is supported by the NSC grant No.98-2918-I-009-06, No.98-2112-M-009-010-MY3, the MOE-ATU program, the NCTS of Taiwan, R.O.C..

Appendix A: RG equations via poor-man’s scaling

In this Appendix, we derive the RG equations in Eq. 4 from the effective Kondo Hamiltonian Eq. 3 in the weak coupling regime via poor-man’s scaling. Based on the scaling dimensions of various Kondo couplings in the weak coupling regime, we focus on the logarithmic derivative of the new dimensionless Kondo couplings $j_{1,2}^{xy,z}$ with respect to the cutoff energy D . First, we focus on the RG

equation for j_1^{xy} :

$$\frac{\partial j_1^{xy}}{\partial \ln D} = (K-1)j_1^{xy} - \mu^{K-1} \frac{\partial J_1^{xy}}{\partial \ln D} \quad (A1)$$

The derivative of J_1^{xy} w.r.t. $\ln D$ is given by:

$$\frac{\partial J_1^{xy}}{\partial \ln D} = \frac{\partial}{\ln D} \int_{D_0}^D d\omega [J_1^{xy} J_1^z \frac{\rho_{1xy,1z}(\omega)}{-\omega} + J_2^{xy} J_2^z \frac{\rho_{2xy,2z}(\omega)}{-\omega}] \quad (A2)$$

Here, $\rho_{1xy,1z}(\omega)$ is the effective electron density of states due to the additional phase correlations associated with J_1^{xy} and J_1^z terms (coming from Luttinger physics) in the effective Kondo couplings, given by²²:

$$\begin{aligned} \rho_{1xy,1z}(\omega) &= \rho_0 \int_0^{|\omega|} dE P_{1\perp 1z}(E), \\ P_{1\perp 1z}(E) &= \frac{1}{2\pi} \int dt \langle \hat{O}_{1\perp 1z}(t) \rangle e^{iEt} \end{aligned} \quad (A3)$$

where ρ_0 is the constant density of states in the non-interacting leads, and

$$\begin{aligned} \langle \hat{O}_{1\perp 1z}(t) \rangle &= \langle e^{-i(\sqrt{4\pi K} - \sqrt{4\pi})\phi_{1(2)}(t)} \rangle \\ &\propto \frac{1}{t^0} = 1 \end{aligned} \quad (A4)$$

since a single un-paired exponential factor does not affect the renormalization of the couplings²². However, $\rho_{2xy,2z}(\omega)$ leads to a non-trivial power-law density of states:

$$\begin{aligned} \rho_{2xy,2z}(\omega) &= \rho_0 \int_0^{|\omega|} dE P_{22}(E), \\ P_{22}(E) &= \frac{1}{2\pi} \int dt \langle \hat{O}_{2\perp 2z}(t) \rangle e^{iEt} \end{aligned} \quad (A5)$$

where

$$\begin{aligned} \langle \hat{O}_{2\perp 2z}(t) \rangle &= \langle e^{-i(\sqrt{\pi/K} - \sqrt{\pi})\theta_1(t)} e^{i(\sqrt{\pi/K} - \sqrt{\pi})\theta_1(0)} \rangle \\ &\times \langle e^{i(\sqrt{\pi/K} - \sqrt{\pi})\theta_2(t)} e^{-i(\sqrt{\pi/K} - \sqrt{\pi})\theta_2(0)} \rangle \\ &\propto \frac{1}{t^{1/K-1}} \end{aligned} \quad (A6)$$

Therefore, we have:

$$\begin{aligned} P_{22}(E) &= c E^{1/K-2} \\ \rho_{2xy,2z}(\omega) &= c' \omega^{1/K-1} \end{aligned} \quad (A7)$$

with c, c' being un-important constants of integration. With the identification $\frac{c'}{1/K-1} D^{1/K-1} \equiv \mu^{1/K-1}$ we obtain

$$\begin{aligned} \frac{\partial j_1^{xy}}{\partial \ln D} &= (K-1)j_1^{xy} - \mu^{K-1} [J_1^{xy} J_1^z + \mu^{1/K-1} J_2^{xy} J_2^z] \\ &= (K-1)j_1^{xy} - j_1^{xy} j_1^z - j_2^{xy} j_2^z \end{aligned} \quad (A8)$$

where we have used the definitions of the new dimensionless couplings $j_1^{xy} = \mu^{K-1} J_1^{xy}$, $j_1^z = J_1^z$, $j_2^{xy,z} = \mu^{1/2(K+1/K)-1} J_2^{xy,z}$. In a similar way, we can derive the remaining RG scaling equations in Eq.4.

Following the same procedures, we are able to derive the RG scaling equations in Eq. 8 from the Hamiltonian Eq. 7 in the strong coupling regime near 2CK fixed point.

Appendix B: RG equations naer 2CK fixed point via ϵ -expansion technique

In this Appendix, we offer an alternative route to Eq. 8 within ϵ -expansion technique.

First, we will prove the renormalization factors $Z_{j^\perp/z}$ and Z_f in Eq. 10. We focus on the 1-loop renormalization of the dimensionless couplings $j_2^{xy} = \mu^\epsilon J_2^{xy}$, and $j_1^z = \mu^{\epsilon'} J_1^z$. Let us look at vertex renormalization of j_1^z first^{23,25}:

$$\tilde{j}_1^z \equiv Z_{j^z}^{-1} j_1^z = j_1^z + (J_2^{xy})^2 \int^D d\omega \frac{\rho_\perp(\omega)}{-\omega} \quad (\text{B1})$$

where

$$\begin{aligned} \rho_\perp(\omega) &= \int^\omega dE P_\perp(E), \\ P_\perp(E) &= \int dt \langle \hat{A}(t) \rangle e^{iEt}, \\ \langle \hat{A}(t) \rangle &= \langle e^{-i\sqrt{4\pi(\frac{1}{K}-1)}\tilde{\theta}(t)} e^{i\sqrt{4\pi(\frac{1}{K}-1)}\tilde{\theta}(0)} \rangle \\ &\propto \frac{1}{t^{2\epsilon}}. \end{aligned} \quad (\text{B2})$$

From above, we find $P(E) \propto E^{2\epsilon-1}$, $\rho_\perp(\omega) = \tilde{c}\omega^{2\epsilon}$. Therefore, Z_{j^z} reads:

$$Z_{j^z} = 1 + \frac{(j_2^{xy})^2/j_1^z}{\epsilon} \quad (\text{B3})$$

with the identification $\mu^\epsilon = \tilde{c}D^\epsilon$. Similarly, we can show that

$$Z_{j^\perp} = 1 + \frac{j_1^z}{\epsilon'} \quad (\text{B4})$$

where the correlator $\langle S^\pm(0)S_z(t) \rangle \propto \frac{1}{t^{2K}}$ is used.

Next, we provide derivation for Z_f . Following Ref.²⁵, the self energy at 1-loop order (see Fig. 5(a) of Ref.²⁵) leads to the following renormalization factor Z_f for impurity fermion:

$$Z_f = 1 + \frac{(J_2^{xy})^2}{4} \int^D d\omega \frac{\rho_\perp(\omega)}{\omega} + \frac{(J_1^z)^2}{8} \int^D d\omega \frac{\rho_z(\omega)}{\omega}, \quad (\text{B5})$$

where

$$\begin{aligned} \rho_\perp(\omega) &= \frac{1}{2\pi} \int dt \langle e^{-i\sqrt{4\pi(\frac{1}{K}-1)}\tilde{\theta}(t)} e^{i\sqrt{4\pi(\frac{1}{K}-1)}\tilde{\theta}(0)} \rangle \\ &\times e^{i\omega t} \propto \omega^{2\epsilon}, \\ \rho_z(\omega) &= \frac{1}{2\pi} \int dt \langle S_z(0)S_z(t) \rangle e^{i\omega t} \propto \omega^{2\epsilon'} \end{aligned} \quad (\text{B6})$$

Plugging Eq. B6 into Eq. B5 and express results in terms of the dimensionless couplings j_2^{xy} and j_1^z , we arrive at:

$$Z_f = 1 + \frac{(j_2^{xy})^2}{8\epsilon} + \frac{(j_1^z)^2}{16\epsilon'}. \quad (\text{B7})$$

With Z_f , Z_{j^\perp} , Z_{j^z} at hand, we now can reproduce the RG scaling equations Eq. 8 via the β -function within the field-theoretical ϵ -expansion approach: $\beta(j_i) \equiv \mu \frac{\partial j_i}{\partial \mu}|_{j_i}$, and $J_2^{xy} = \frac{\mu^{-\epsilon} Z_{j^\perp}}{Z_f} j_2^{xy}$, $\tilde{j}_1^z = \frac{\mu^{-\epsilon'} Z_{j^z}}{Z_f} j_1^z$.

Appendix C: Stability analysis of 1CK and 2CK fixed points for a Kondo dot couples to two Luttinger liquid leads

In this Appendix, we generalize the argument in Section E. to address the stability of the 1CK and 2CK fixed points for a Kondo dot couples to two Luttinger liquid leads. The Kondo Hamiltonian in the bosonized form is given by¹²:

$$\begin{aligned} H_K &= J_1^z S_z \partial_x \theta_s \\ &+ J_2^z S_z \sin(\sqrt{2\pi}\theta_a) \sin(\sqrt{\frac{2\pi}{K}}\phi_a) \\ &+ J_1^{xy} [S^+ e^{i\sqrt{2\pi}\theta_s} \cos(\sqrt{2\pi}\theta_a) + h.c.] \\ &+ J_2^{xy} [S^+ e^{i\sqrt{2\pi}\theta_s} \cos(\sqrt{\frac{2\pi}{K}}\phi_a) + h.c.] \end{aligned} \quad (\text{C1})$$

where we define the above boson fields via standard bosonization¹²: $\phi_{s/a} \equiv \frac{\phi_1 \pm \phi_2}{\sqrt{2}}$, $\phi_{1(2)} \equiv \phi_{1(2)L} + \phi_{1(2)R}$, $\phi_{i,L(R)} = \frac{\phi_{i,L(R)}^+ + \phi_{i,L(R)}^-}{\sqrt{2}}$, $\theta_{s/a} \equiv \frac{\theta_1 \pm \theta_2}{\sqrt{2}}$, $\theta_{1(2)} \equiv \theta_{1(2)L} + \theta_{1(2)R}$, $\theta_{i,L(R)} = \frac{\phi_{i,L(R)}^+ - \phi_{i,L(R)}^-}{\sqrt{2}}$. In the weak coupling limit, the scaling dimensions for the four Kondo couplings are: $[J_1^{xy}] = [J_1^z] = 1$, $[J_2^{xy}] = [J_2^z] = \frac{1}{2} + \frac{1}{2K}$. The RG scaling equations in this limit are well understood.

We can access to the strong coupling regime by the Emory-Kivelson canonical transformation: $U = e^{-i\sqrt{2\pi}S_z\theta_s}$. The transformed Kondo Hamiltonian is given by:

$$\begin{aligned} H_K &= \tilde{J}_1^z S_z \partial_x \theta_s \\ &+ J_2^z S_z \sin(\sqrt{2\pi}\theta_a) \sin(\sqrt{\frac{2\pi}{K}}\phi_a) \\ &+ J_1^{xy} S_x \cos(\sqrt{2\pi}\theta_a) \\ &+ J_2^{xy} S_x \cos(\sqrt{\frac{2\pi}{K}}\phi_a) \end{aligned} \quad (\text{C2})$$

where $\tilde{J}_1^z = J_1^z - 2\pi v_F$. Near strong coupling regime $J_1^z \approx \mathcal{O}(1)$, J_1^{xy} is the most relevant term with scaling dimension $[J_1^{xy}] = 1/2$. Near 2CK fixed point ($J_1^{xy} \rightarrow \infty$) θ_a is pinned at a constant value, leading to the same scaling dimensions for $J_2^{xy,z}$: $[J_2^{xy,z}] = \frac{1}{2K}$. This implies that the 2CK fixed point is stable for $K < 1/2$ as J_2^{xy} term is always irrelevant while as $J_1^{xy,z}$ become large. However, for $K > 1/2$ the 2CK fixed point is unstable towards the 1CK fixed point as $J_2^{xy,z}$ terms becomes relevant, and all four Kondo couplings flow to the strong coupling fixed point.

Now, we turn our attention to the stability analysis of the 1CK fixed point. For $K = 1$ (non-interacting leads), it is known that 1CK fixed point is stable⁸. For $K < 1$, however, we need to analyze the effective Hamiltonian δH_{1CK} near 1CK fixed point. Via the same argument as in Sec. V., we find the dominating term is given by the on-site Coulomb interaction:

$$\delta H_{1CK} \approx H_u = u(c_{e\sigma}^\dagger(a)c_{e\sigma}(a) - 1)^2. \quad (C3)$$

There are two terms in H_u which may drive the system away from 1CK fixed point: (i). the two-particle spin-flip backscattering term: $H_\sigma = g_\sigma \psi_{R\uparrow}^\dagger \psi_{R\downarrow} \psi_{L\downarrow}^\dagger \psi_{L\uparrow} + h.c.$ (ii). the Umklapp term which plays a role when $k_f = \frac{\pi}{2a}$: $H_{um} = g_{um} e^{i4k_f a} \sum_{\sigma, \sigma'=\uparrow, \downarrow} \psi_{L\sigma}^\dagger \psi_{R\sigma} \psi_{L\sigma'}^\dagger \psi_{R\sigma'} + h.c..$ Via bosonization $\psi_{R(L)}^\sigma = \frac{1}{\sqrt{2\pi a}} e^{\pm i(\sqrt{4\pi}\phi_{R(L)}^\sigma(x) + k_F x)}$, the above two terms have the following forms:

$$\begin{aligned} H_\sigma &\propto g_\sigma \cos(\sqrt{8\pi}\phi_{sf}), \\ H_{um} &\propto g_{um} \cos(\sqrt{8\pi K}\phi_f) \end{aligned} \quad (C4)$$

where we have performed the following basis change from $(\phi_L^\uparrow, \phi_L^\downarrow, \phi_R^\uparrow, \phi_R^\downarrow)$ to $(\phi_c, \phi_f, \phi_s, \phi_{sf})$ ²²: $\phi_c \equiv \frac{\phi_{cL} + \phi_{cR}}{\sqrt{2}}$, $\phi_f \equiv \frac{\phi_{cL} - \phi_{cR}}{\sqrt{2}}$, $\phi_s \equiv \frac{\phi_{sL} + \phi_{sR}}{\sqrt{2}}$, $\phi_{sf} \equiv \frac{\phi_{sL} - \phi_{sR}}{\sqrt{2}}$, $\phi_{cL(R)} \equiv \frac{\phi_{L(R)}^\uparrow + \phi_{L(R)}^\downarrow}{\sqrt{2}}$, $\phi_{sL(R)} \equiv \frac{\phi_{L(R)}^\uparrow - \phi_{L(R)}^\downarrow}{\sqrt{2}}$. The scaling dimension of g_σ and g_{um} can be obtained in a similar manner: $[g_\sigma] = 2 > 1$, $[g_{um}] = 2K$. This implies that g_σ term is always irrelevant; while g_{um} term is irrelevant for $K > 1/2$, and it becomes relevant for $K < 1/2$ where the relevant coupling g_{um} term is expected to drive the system away from the 1CK fixed point.

- ¹ Quantum phase transitions, Cambridge University press (2000); S. L. Sondhi, S. M. Girvin, J. P. Carini, and D. Shahar, Rev. Mod. Phys. **69**, 315 (1987)
- ² K. Le Hur, Phys. Rev. Lett. **92**, 196804 (2004).
- ³ A. Furusaki, K.A. Matveev, Phys. Rev. Lett. **88**, 226404 (2002).
- ⁴ Gergely Zarand, Chung-Hou Chung, Pascal Simon and Matthias Vojta, Phys. Rev. Lett. **97**, 166802 (2006); C.H. Chung, W. Hofstetter, Phys. Rev. B **76**, 045329 (2007); Chung-Hou Chung, Gergely Zarand, and Peter Woelfle, Phys. Rev. B **77**, 035120 (2008).
- ⁵ Eran Sela, Ian Affleck, Phys. Rev. Lett. **102**, 047201 (2009).
- ⁶ Chung-Hou Chung, Karyn Le Hur, Matthias Vojta, Peter Woelfle, Phys. Rev. Lett. **102**, 216803 (2009); C.-H. Chung, K.V.P. Latha, K. Le Hur, M. Vojta, P. Woelfle, Phys. Rev. B, **82**, 115325 (2010).
- ⁷ Stefan Kirchner, Qimiao Si, Phys. Rev. Lett. **103**, 206401 (2009).
- ⁸ A.C. Hewson Kondo problems to heavy fermions, Cambridge University Press, Cambridge, 1997.
- ⁹ D. Goldhaber-Gordon, H. Shtrikman, D. Mahalu, D. Abusch-Magder, U. Meirav, and M. A. Kastner, Nature London **391**, 156 1998 ; W. G. van der Wiel, S. De Franceschi, T. Fujisawa, J. M. Elzerman, S. Tarucha, and L. P. Kouwenhoven, Science, **289**, 2105 2000; L. Kouwenhoven and L. Glazman, Phys. World **14**, 33 (2001).
- ¹⁰ D.L. Cox, A. Zawadowski, Advances in Physics, **47**, 599 (1998); P. Noziere, A. Blandin, J. Physique **41**, 193 (1980).
- ¹¹ R. M. Potok, I. G. Rau, H. Shtrikman, Y. Oreg, and D. Goldhaber-Gordon, Nature London **446**, 167 2007.
- ¹² M. Fabrizio and A.O. Gogolin, Phys. Rev. B **51**, 17827 (1995).
- ¹³ E. Kim, arXiv:condmat/0106575 (unpublished).
- ¹⁴ M.Z. Hasan, C.L. Kane, Rev. Mod. Phys. **82**, 3045 (2010).
- ¹⁵ Fu, L., C.L. Kane, Phys. Rev. B **76**, 045302 (2007); B.A. Bernevig, T.A. Hughes, S.C. Zhang, Science **314**, 1757 (2006).
- ¹⁶ Hsieh, D.; D. Qian, L. Wray, Y. Xia, Y. S. Hor, R. J. Cava, M. Z. Hasan, Nature **452**, 970 (2008).
- ¹⁷ K.T. Law, C.Y. Sheng, Patrick A. Lee, and T.K. Ng, Phys. Rev. B **81**, 041305(R) (2010).
- ¹⁸ I. Affleck and A.W.W. Ludwig, Phys. Rev. Lett. **67**, 161 (1991).
- ¹⁹ P. Fendley, F. Lesage, and H. Saleur, J. Stat. Phys. **79**, Nos. 5/6, 799 (1995).
- ²⁰ A. O. Gogolin, A. A. Nersesyan, and A. M. Tsvelik, Bosonization and Strongly Correlated Systems (Cambridge University Press, Cambridge, 1998); T. Giamarchi, Quantum Physics in One Dimension (Oxford University Press, Oxford, 2004).
- ²¹ V. J. Emery and S. Kivelson, Phys. Rev. B **46**, 10812 (1992).
- ²² Jefferey C.Y. Teo, C.L. Kane, Phys. Rev. B **79**, 235321 (2009).
- ²³ S. Florens, P. Simon, S. Andergassen, and D. Feinberg, Phys. Rev. B **75**, 155321 (2007).
- ²⁴ L. Fritz, M. Vojta, Phys. Rev. B **70**, 214427 (2004).
- ²⁵ Lijun Zhu, Qimiao Si, Phys. Rev. B **66**, 024426 (2002).
- ²⁶ C. Wu, B.A. Bernevig, and S.C. Zhang, Phys. Rev. Lett., **96** 106401, (2006).